Proc. Natl. Acad. Sci. USA
Vol. 96, pp. 3606–3610, March 1999
Biochemistry

Cytoplasmic RNA modulators of an inside-out signal-transduction cascade

MICHAEL BLIND*, WALDEMAR KOLANUS†‡, AND MICHAEL FAMULOK*‡

*Institut für Biochemie and †Laboratorium für Molekulare Biologie–Genzentrum, Ludwig-Maximilians-Universität Munich, Feodor-Lynen-Strasse 25, 81377 Munich, Germany

Communicated by Rolf Huisgen, University of Munich, Munich, Germany, January 25, 1999 (received for review December 14, 1998)

ABSTRACT **A vaccinia virus-based RNA expression system enabled high-level cytoplasmic expression of RNA aptamers directed against the intracellular domain of the β2 integrin LFA-1, a transmembrane protein that mediates cell adhesion to intercellular adhesion molecule-1 (ICAM-1). In two different cell types, cytoplasmic expression of integrin-binding aptamers reduced inducible cell adhesion to ICAM-1. The aptamers specifically target, and thereby define, a functional cytoplasmic subdomain important for the regulation of cell adhesion in leukocytes. Our approach of aptamer-controlled blocking of signaling pathways *in vivo* could potentially be applied wherever targeted modulation of a signal-transduction cascade is desired.**

To understand or control the functions of individual intracellular protein subdomains *in vivo*, general strategies to create and employ specific modulators of macromolecular interactions are needed. Therefore, a major biological and medical challenge is to identify such selective tools (1–5). Here we describe an approach based on cytoplasmic domain recognition of the β2 integrin LFA-1 by synthetic ligand-binding RNA aptamers (6–11) isolated from a combinatorial RNA library, their high-level expression in the cytoplasm of leukocytes, and investigations into their biological effects *in vivo*.

Integrins are versatile heterodimeric transmembrane proteins that mediate adhesive interactions with extracellular matrix and cell-specific counterreceptors and are implicated in diverse biological processes, including apoptosis, cell-cycle regulation, cell migration, blood clotting, memory, and leukocyte function (12). The cytoplasmic domains of integrins play important roles in regulating cell adhesion (13, 14), probably by linking signaling events inside the cell to the extracellular domains, but the precise mechanisms are unclear. The β2 integrin LFA-1 (αLβ2, CD11a/CD18) mediates adhesion of leukocytes in immune and inflammatory responses by binding to cellular ligands (15), the intercellular adhesion molecules ICAM-1, -2, or -3. A large body of data implicates the cytoplasmic domain of the β2 chain in the regulation of LFA-1-mediated adhesiveness, presumably through its interactions with intracellular proteins and/or the membrane-proximal cytoskeleton (16), and some candidate cytoplasmic ligands have recently been identified (17–20). Further insights into these mechanisms may be gained by specifically inhibiting the LFA-1-mediated inside-out signal transduction *in vivo*. Our objectives were the selection of aptamers that bind to the cytoplasmic domain of CD18, the development and application of a system allowing high-level expression of aptamers within the cytoplasm of leukocytes, and investigation into their biological effects in the context of the living cell.

The publication costs of this article were defrayed in part by page charge payment. This article must therefore be hereby marked "*advertisement*" in accordance with 18 U.S.C. §1734 solely to indicate this fact.

PNAS is available online at www.pnas.org.

MATERIALS AND METHODS

***In Vitro* Selection of CD18-Binding RNA Aptamers.** An RNA library with a complexity of 5×10^{14} different molecules was synthesised by *in vitro* T7-transcription from the PCR-amplified synthetic DNA pool MF76.1: 5′-TC*TAATACGACTCACTATA*GG*GCGCTA*AGTCCTCGCTCA-N40-ACGCGCGACTC**GGATCC**T-3′; primer MF39.1: 5′-TC*TAATACGACTCACTATA*GG*GCGCTA*A GTCCTCGCTCA-3′ (*italic*, T7-promotor; **bold**, *Bam*HI restriction site); primer Mic20.1: 5′-GTA**GGATCC**GAGTCGCGCGT-3′ (**bold**, *Bam*HI restriction site) as described (21). CNBr-activated Sepharose was derivatized with synthetic peptides (CD18cyt, MF2G) or blocked with Tris·HCl (pH 8.0) alone according to the manufacturer's protocol. For the preselection, 50–75 μl of either Tris-blocked or MF2G-derivatized Sepharose was incubated with 2–3 nmol α-^{32}P-labeled RNA in 150 μl of binding buffer (buffer B: 4.3 mM K_2HPO_4, 1.4 mM NaH_2PO_4, 150 mM NaCl, 1.0 mM $MgCl_2$, 0.1 μM $CaCl_2$) for 1 h at 23°C. The slurry was transferred into a plastic column and eluted in small fractions (75 μl) with buffer B. For the actual selection, the initial four fractions were precipitated and incubated with 25–50 μl of CD18cyt-Sepharose (4.5 mg/ml gel) in 100 μl of buffer B for 1 h at 23°C. Removal of nonbinding RNAs was achieved by washing with 200 Sepharose-volumes of binding buffer (5–10 ml). Bound RNAs were eluted by washing with buffer B adjusted to 6 M guanidinium-HCl. Eluted fractions were quantified by Cherenkov counting, ethanol-precipitated in the presence of 10–20 μg of glycogen, and reverse-transcribed as described (22); cDNA was PCR-amplified, followed by *in vitro* transcription. For cycle one, 29 nmol of RNA and 120 μl of CD18cyt-Sepharose in a total volume of 475 μl were used. After cycle 11, binding sequences were PCR-amplified with primers Mic20.1 and SK40.4 (5′-TC*TAATACGACTCACTATA*GGG**CTGCAG**AGTCCTCGCTCA-3′; *italic*, T7-promotor; **bold**, *Pst*I restriction site) to introduce a *Pst*I restriction site, cloned, and sequenced as described (22).

Transfection of Cells with vaccinia T7 (vT7) and vaccinia T7-RNA (vTR). Jurkat E6 and peripheral blood mononuclear cells (PBMC) were isolated according to standard protocols (23). The sequence of the T7-RNA expression cassette (TR), shown here without inserted aptamer (5′-**GTTAAC-GCATG-C***TAATACGACTCACTATA*gggagaccacaacggttt**cccGGG**CGCAAGTT**ACTAGT-TGGCCA-AGATCT-TAATTAA**tagcataacccttggggcctctaaacgggtcttgaggggttttttgct**GTCGAC-GCGG-CCGC**-3′; **bold**, restriction sites in the order in which they appear *Hpa*I, *Sph*I, *Xba*I, SpeI, *Bal*I, *Bgl*II, *Pac*I, *Sal*I, and *Not*I; *italic,* T7-promotor; lower case, stabilizing stem-loops) was inserted into the vector pTkg (24, 25) via *Hpa*I and *Not*I restriction sites, resulting in the transfer TR vector. Aptamer-coding sequences were inserted via the *Xba*I and *Pac*I restric-

Abbreviations: ICAM-1, intercellular adhesion molecule 1; PMA, phorbol 12-myristate 13-acetate; PBMC, peripheral blood mononuclear cells; PH, plextrin homology.

‡To whom reprint requests should be addressed. e-mail: Famulok@lmb.uni-muenchen.de or Kolanus@lmb.uni-muenchen.de.

tion sites (TR-aptamer; for an overview see Fig. 2*A*). The construction of the expression cassette with synthetic oligonucleotides by PCR and the insertion of the aptamer-encoding sequences via *Xba*I and *Pac*I restriction sites will be described elsewhere. Vaccinia expression constructs (vTR-aptamer) were derived via recombination between the TR vector and wild-type vaccinia virus (WR strain), high-titer virus stocks were generated as described (26), and double infections with recombinant vaccinia viruses and a vaccinia virus coding for T7-RNA polymerase (vT7) were carried out as described previously (20). Briefly, 2×10^6 cells were collected by centrifugation, washed with PBS, resuspended in 300 μl of RPMI medium 1640; 100–150 μl of each virus stock (multiplicity of infection of $\approx$10 plaque-forming units per cell, sonicated for 10 s) was added and incubated for 2 h at 37°C, followed by addition of 4 ml of RPMI/10% fetal calf serum and additional incubation for between 1 and 7 h.

Dot Blot Analysis of Cytoplasmatic Aptamers. Approximately 4×10^6 Jurkat E6 cells were infected with vaccinia viruses expressing aptamer RNA and T7-RNA polymerase. RNA was isolated as described (26) and blotted onto a Hybond N membrane (DuPont/NEN) according to the manufacturer's protocol. Hybridization of virus-expressed RNA was carried out for 1 h by incubation of cellular RNA in prehybridization buffer (5× SSC, 0.1% SDS, 5× Denhardt's reagent, 5% dextran sulfate, 100 μg/ml tRNA) at 55°C, followed by incubation in the presence of 20 pmol of radiolabeled probe MicTR1/28.1 (5′-CAAAAAACCCCTCAAG ACCCGTTTAGAG-3′) in a total volume 4.0 ml for 1 h. Dot-blots were then washed with $\approx$20 ml of 2× SSC/0.1% SDS (2×)/1× SSC/0.1% SDS (2×) and 0.5× SSC/0.1% SDS (2×) at 55°C for 30 min and quantified by PhosphorImaging.

Gel Shift Assays. Jurkat E6 cells (4×10^7) were lysed in 400 μl of lysis buffer (PBS, 0.5% Triton X-100, 0.5 μg/ml aprotinin, 0.5 μg/ml leupeptin, 1 mM PMSF, and 1 mM $MgCl_2$) and incubated at 0°C for 20 min. Nuclei were removed by centrifugation at 3,000 × *g* for 10 min, and the supernatant was clarified by centrifugation at 10,000 × *g* for 10 min. To 3 μl of this lysate, 2 μg of purified mAb (MHM23, OKT3) or 2 μl of ascites fluid (MEM170) were added and adjusted to 1× PBS in a total volume of 7 μl. After incubation at 0°C for 2–3 h, 5 μl of PBS containing 3 mM DTT, 1 mM $MgCl_2$, 30 units of RNasin, 75–120 μM tRNA, 20% glycerol, and 7.5 μg of BSA were added, and the mixture was incubated at 0°C for 15 min. Following incubation, 30–60 fmol of 5′-^{32}P-labeled TR-aptamer in 3 μl of PBS and 1 mM $MgCl_2$, heated to 95°C for 30s and cooled to 23°C for 10 min, was added, and the mixture was incubated at 23°C for 30 min. The lysate/aptamer/antibody mixture was loaded onto a native 4.5% polyacrylamide gel (acrylamide/bisacrylamide, 60:1) containing 2% glycerol and electrophoresed at 150 V for 2.5 h in 0.25× TAE electrophoresis buffer. Gel shifts employing synthetic biotinylated peptides were performed as follows: 5 μl of 3 nM radiolabeled aptamer RNA in PBS (pH 7.4) was heated to 95°C for 30 s and renatured for 10 min at 23°C. Biotinylated peptide was incubated with 2 mg/ml streptavidin in 20 mM Tris·HCl (pH 7.4) in a total volume of 6 μl. To this solution, a pre-mix was added to adjust the concentrations in the final 20 μl reaction volume to 1× PBS, 1 mM DTT, 1 mM $MgCl_2$, 7.5% glycerol, 2.5 mg/ml BSA, 40 μM tRNA, and 2 units/μl RNasin, and the mixture was preincubated for 20 min at 23°C. The aptamer solution (5 μl) was added, incubated for 20 min at 23°C, and electrophoresed on a native 6% polyacrylamide gel as described above.

Adhesion Assays. The ICAM-1–Rg fusion protein was expressed in COS-7 cells, purified from culture supernatants by protein A-Sepharose, eluted, resuspended in PBS, and coated onto plastic dishes as described (20). Jurkat cells or PBMC (2×10^6) were infected with recombinant vaccinia viruses and incubated for 4–8 h at 37°C. After centrifugation, cells were resuspended in RPMI medium 1640 and incubated for 5 min at 37°C with or without the addition of 40 ng/ml phorbol 12-myristate 13-acetate (PMA). Cells were subsequently allowed to adhere to ICAM-1-Rg coated dishes at 37°C for 30 min and the bound fraction was determined with the aid of an ocular reticle.

RESULTS AND DISCUSSION

The RNA library was subjected to 11 cycles of *in vitro* selection by binding to a 46-mer peptide corresponding to the complete cytoplasmic domain of CD18 (CD18cyt) immobilized on a Sepharose matrix (Fig. 1*A*). From the enriched pool, 80 aptamers were cloned and sequenced. Based on sequence motifs, these aptamers can be subdivided into either four classes or orphan sequences without any obvious relationship to each other. *In vitro* binding to the CD18cyt-peptide was confirmed for several clones (Fig. 1*B*) by using column-binding assays (data not shown). The binding affinity of monoclonal aptamers to the immobilized CD18cyt-peptide was between 500 and 1,000 nM. No binding of individual aptamers to underivatized Sepharose was observed.

Four sequences were chosen for the cytoplasmic expression studies. Three of them, D20, D28, and D31, are CD18-binders, and the fourth sequence, D42, is a nonbinding negative control sequence of the same length and with primer-binding sites identical to the specific aptamers (Fig. 1*B*). First, a TR vector was constructed where the T7 promoter is located upstream of aptamer-coding DNA inserted between 5′ and 3′ stem-loop structures that serve as RNA-stabilizing motifs and are required for correct termination of the T7 transcripts (27) (Fig. 2*A*). The resulting transcripts are called TR-aptamers. As negative controls, we also used a TR vector lacking the aptamer sequence and one that expressed the nonbinding negative control sequence TR-D42. Importantly, TR-aptamers were confirmed to exhibit the same *in vitro* binding behavior to the CD18cyt-peptide when expressed in the context of the flanking stem-loop structures (data not shown).

Cytoplasmic RNA expression relies on coinfection of cells with two recombinant vaccinia viruses (27). One virus, vT7,

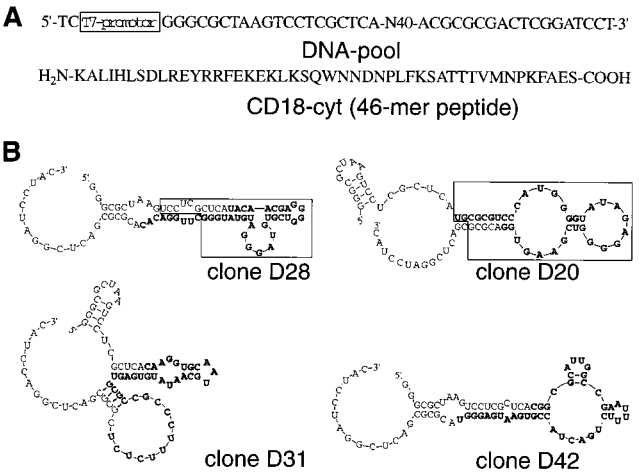

FIG. 1. Selection and characterization of CD18cyt-specific RNA aptamers. (*A*) Construction of the synthetic DNA pool and primary 46-mer amino acid sequence of the complete cytoplasmic domain of β2-integrin (CD18cyt), immobilized to Sepharose and used in the selection. (*B*) Sequences and predicted secondary structures of individual aptamer clones D20, D28, D31, and D42. Nucleotides shown in **bold** are part of the randomized region. The boxed aptamer region in clones D28 and D20 were shown in a damage-selection experiment to be minimal requirements for retaining CD18cyt-binding capacity. The sequence D42 was used as a negative control; this aptamer does not show any detectable binding to CD18cyt.

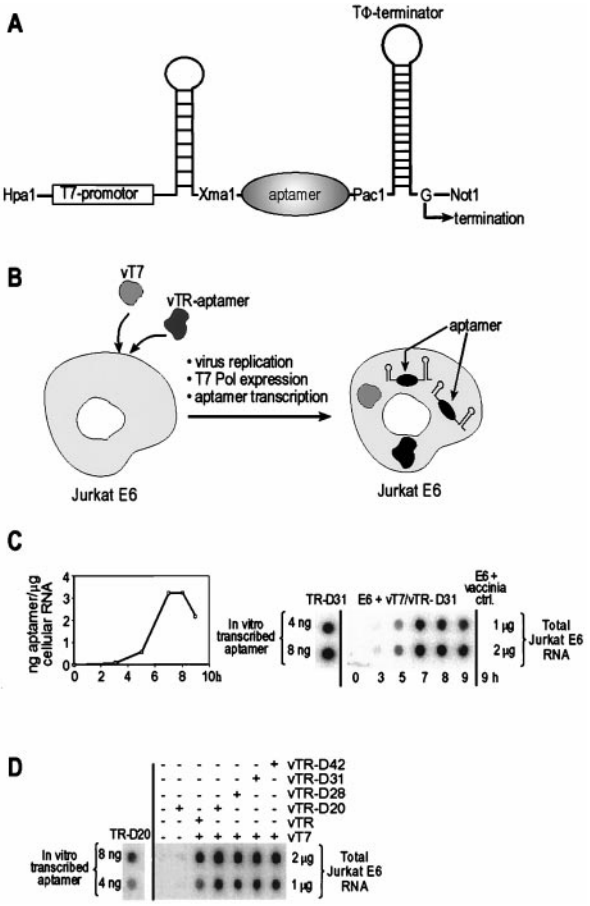

FIG. 2. RNA aptamer expression system based on double infection with recombinant vaccinia viruses. (*A*) Design of the T7-RNA expression cassette. (*B*) Schematic representation of the vaccinia virus-based cytoplasmatic RNA aptamer expression system. (*C*) Course of the expression of TR-encoded aptamer in vT7-coinfected Jurkat E6 cells shown by a representative dot-blot analysis for aptamer TR-D31 (*Right*). Maximum levels of aptamer expression are seen 7 h postinfection. Quantification (*Left*) was done as follows: total cellular RNA was isolated, transferred to the blotting membrane and hybridized with 5′-^{32}P-labeled oligonucleotide complementary to the 3′-stabilizing stem-loop structure present in all TR constructs. For comparison and quantification, *in vitro*-transcribed aptamer TR-D20 was treated in the same way. D, Dot blot analysis and quantification of maximally expressed aptamer RNA. Each dot was quantified on a PhosphorImager. Quantification was done as described for *C*.

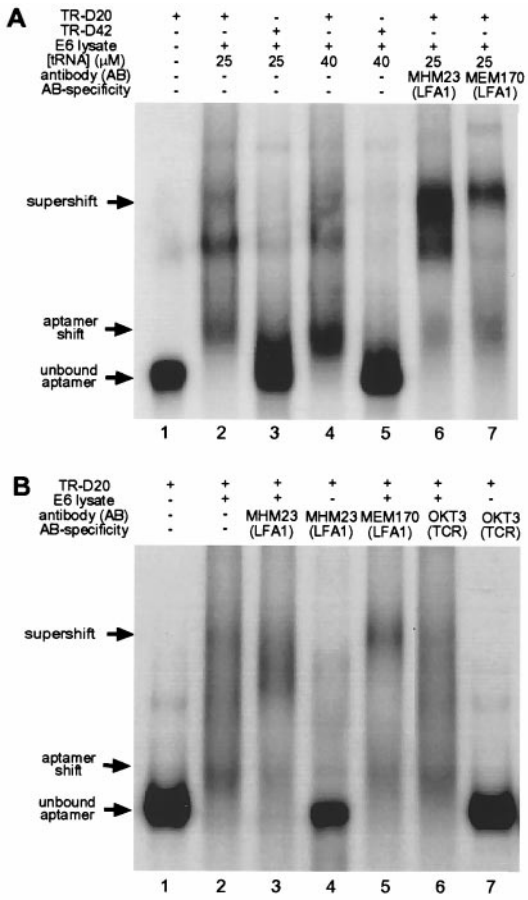

FIG. 3. Gel mobility-shift assays of endogenous CD18 contained in Jurkat E6 cell lysates bound to its cognate aptamer TR-D20. (*A*) Gel-shift experiment 1. Lane 1, free TR-D20 aptamer RNA; lane 2, shifted band obtained in presence of Jurkat E6 lysate and 25 µM nonspecific competitor tRNA; lane 3, no shift obtained with negative control sequence TR-D42; lane 4, same as lane 2 with 40 µM nonspecific competitor tRNA; lane 5, same as lane 3 with 40 µM nonspecific competitor tRNA; lane 6, specific supershifted band obtained in the presence of antibody MHM23, which recognizes the β2-extracellular domain of LFA-1; lane 7, specific supershifted band obtained in the presence of antibody MEM170, which recognizes the extracellular domain of the αL-subunit of LFA-1. The band pattern may reflect aptamer/integrin complexes of different stoichiometry. (*B*) Gel-shift experiment 2 with additional controls. All gel-shift experiments were performed in the presence of 30 µM tRNA as a nonspecific competitor. Lane 1, free TR-D20 aptamer RNA; lane 2, shifted band obtained in presence of Jurkat E6 lysate; lane 3, specific supershifted band obtained in the presence of antibody MHM23; lane 4, no shifted aptamer obtained in the absence of Jurkat E6 cell lysate under conditions identical to those in lane 3; lane 5, specific supershifted band obtained in the presence of antibody MEM170; lane 6, no supershift obtained in the presence of antibody OKT3 directed against the T cell receptor. The experimental conditions are otherwise the same as in lane 2; lane 7, no shifted aptamer obtained in the absence of Jurkat E6 cell lysate under conditions identical to those in lane 6.

codes for the bacteriophage T7 RNA polymerase; the other, vTR-aptamer, encodes the sequence of the TR-aptamer and is derived from homologous recombination between vaccinia virus and the TR-aptamer vector. The course of RNA expression after coinfection of a Jurkat E6 cell line with vT7 and vTR-D31 is shown in Fig. 2*C*. Maximal amounts of RNA are reached 7 h postinfection as quantified by dot-blot analysis by using a DNA hybridization probe complementary to the 3′ terminus of the aptamer expression cassette. Analysis of all TR transcripts *in vivo* at this peak revealed comparable aptamer RNA levels of roughly 10^6 copies per cell, but only in the presence of vT7 (Fig. 2*D*).

Before investigating the biological effects of aptamer expression, we had to confirm that the aptamers are also able to specifically bind endogenous LFA-1. This was demonstrated by incubating radiolabeled aptamers transcribed *in vitro* from TR-aptamer vectors with crude cytoplasmic lysate from Jurkat E6 cells and subsequent gel electrophoresis under native conditions. As shown in Fig. 3 in two representative experiments, this resulted in a pattern of shifted bands that were aptamer-specific. Aptamer TR-D20 shows a band pattern with significantly reduced electrophoretic mobility (Fig. 3*A*, lanes 2 and 4) in comparison with the negative controls of lysate-free RNA (lane 1) and nonbinding TR-D42 (lanes 3 and 5) in the presence of a 10^4-fold excess of tRNA as a nonspecific competitor. To test whether the shifts were also LFA-1-specific, we performed a supershift analysis with two independent LFA-1-specific antibodies (MHM23 and MEM170) directed against the extracellular domain of the β- and α-subunits of LFA-1, respectively, and the antibody OKT3, which recognizes the ε-chain of the T cell antigen receptor as a negative control. Addition of either MHM23 or MEM170 (Fig.

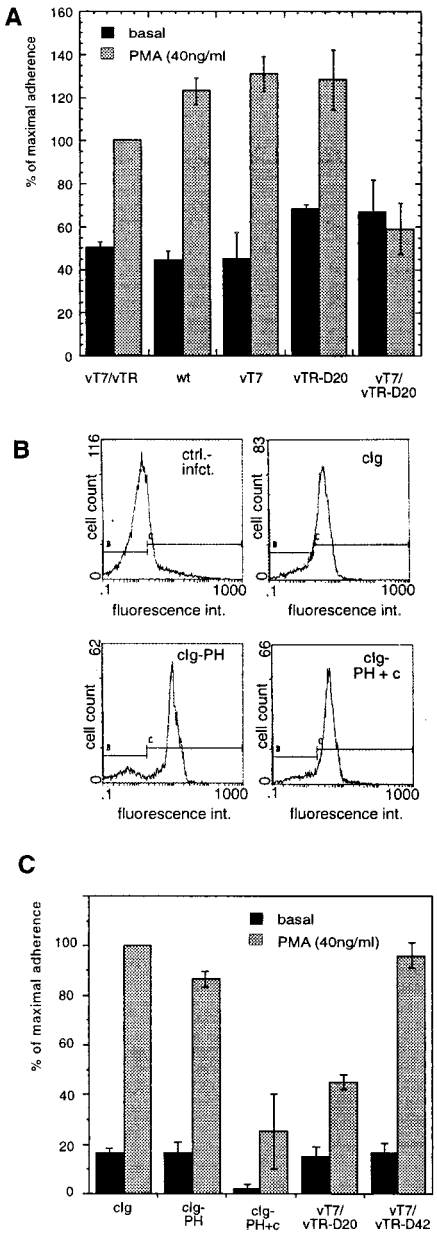

FIG. 4. Inhibition of PMA-stimulated cell adhesion as a function of aptamer expression. (*A*) The CD18cyt binder TR-D20 reduces phorbol ester-activated Jurkat cell adhesion to ICAM-1. Jurkat E6 cells infected with recombinant vaccinia viruses were allowed to adhere to plastic dishes coated with a recombinant ICAM-1 chimera as described in *Material and Methods*. Jurkat E6 cell adhesion to ICAM-1 was superinducible by PMA in the presence of several control viruses (vT7/vTR, wild-type vaccinia virus, vT7, and vTR-D20). However, induction of CD18cyt-specific aptamer expression (vT7/vTR-D20, *Right*) reduced PMA-stimulated Jurkat E6 cell adhesion but not basal adhesion. These results were independently reproduced at least three times. Percentage reflects values normalized to stimulated vT7/vTR double infection, which was set to 100%. (*B*) Human PBMC are good targets for protein overexpression by recombinant vaccinia viruses. Cytoplasmic Ig (cIg) fusions of cytohesin-1 subdomains were detected with the help of an FITC-conjugated anti-human Ig antibody preparation in permeabilized PBMC. *Upper Left*, control infection, no recombinant molecules expressed; *Upper Right*, cIg-domains alone; *Lower Left*, cIg-PH; *Lower Right*, cIg-PH+c-domain. (*C*) TR-D20 specifically reduces PMA-stimulated adhesion of PBMC to ICAM-1. Aptamers or control proteins were expressed in PBMC by recombinant vaccinia viruses as described above. PMA-stimulated adhesion of these cells to ICAM-1 was equivalent when the TR-D42 aptamer, cIg, or cIg-PH control proteins were expressed, but stimulated cell adhesion was dramatically reduced after expression of the intact PH + c-domain of cytohesin-1 (cIg-PH+c) or of the TR-D20 aptamer.

3*A*, lanes 6 and 7) resulted in a supershifted band. In Fig. 3*B* again both LFA-1-specific antibodies MHM23 and MEM170 (lanes 3 and 5) show the supershifted bands, whereas no supershift was obtained with the noncognate antibody OKT3 (lane 6). The experiments shown in lanes 4 and 7 establish that the aptamer TR-D20 has no direct affinity to either the specific antibody MHM23 or the nonspecific antibody OKT3. When the gel-shift experiment shown in lane 2 was repeated in the presence of 2 μM unlabeled TR-D20 aptamer as a specific competitor, all radiolabeled TR-D20 RNA migrated at the level of unbound RNA (data not shown). Analogous results were obtained with TR-D28 and TR-D31, showing that the aptamers recognize endogenous CD18 in crude cell lysates with remarkable specificity.

To test whether the cytoplasmic expression of CD18-specific aptamers has an effect on the biological activity of this integrin, we performed adhesion assays with Jurkat E6 cells or with PBMC (23). The cells were infected with vaccinia viruses encoding CD18-specific aptamers or various control sequences, and binding of these cells to an important ligand of LFA-1, the ICAM-1 molecule, was assessed *in vitro*. This system has a further level of control, because we knew that aptamer expression absolutely depends on coinfection of cells with a virus expressing T7 polymerase (Fig. 2*D*). Fig. 4*A* shows that infected Jurkat E6 cells displayed considerable background adhesion to ICAM-1, but this was nonetheless superinducible by PMA, a well known promoter of LFA-1-mediated leukocyte adhesion (15). Notably, whereas the TR without insert and single infections with wild-type vaccinia virus, vT7, or vTR-D20 had almost no effect, expression of the TR-D20 aptamer in Jurkat cells resulted in an almost complete block of inducible adhesion.

The reproducibility and extension of the method to other systems was tested by performing similar studies with human PBMC, which although normally difficult to transfect, proved

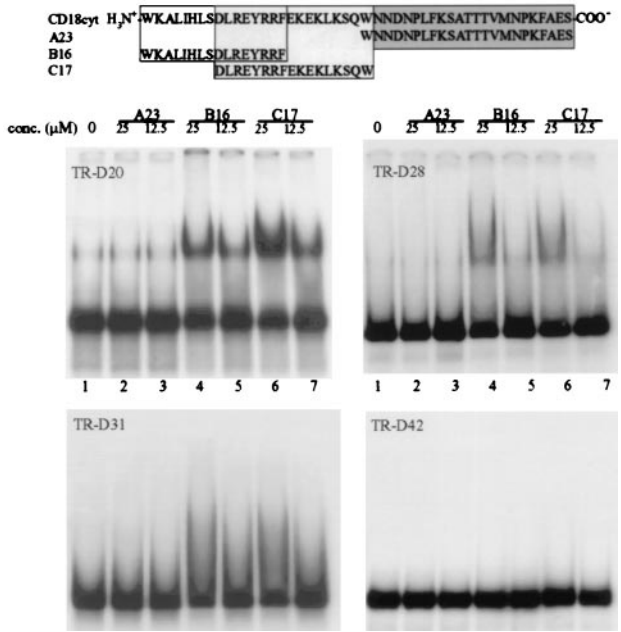

FIG. 5. Mapping of the binding site of aptamers TR-D20, TR-D28, and TR-D31 and the negative control sequence TR-D42 on CD18cyt by using synthetic biotinylated peptide fragments. All gel shifts were carried out in the presence of 25 μM streptavidin to enhance separation of shifted vs. nonshifted RNA. Gel-shift experiments were performed in the presence of 4 nM radiolabeled RNA and 40 μM nonspecific tRNA competitor. Lane 1, free aptamer in the presence of 25 μM streptavidin and 40 μM unspecific competitor tRNA; lanes 2, 4, and 6 or 3, 5, and 7, same as lane 1 in presence of 25 μM or 12.5 μM, respectively, peptides A23 (lanes 2 and 3), B16 (lanes 4 and 5), and C17 (lanes 6 and 7).

to be superb targets for transient gene expression mediated by recombinant vaccinia viruses. A flow cytometric analysis of vaccinia-expressed control proteins, subdomain derivatives of cytohesin-1, clearly shows that Ig fusion proteins with the cytohesin-1 plextrin homology (PH) domain (cIg-PH) and the PH+c-domains (cIg-PH+c), or the isolated Ig portion itself (cIg) were all expressed at equally high levels in human PBMC (Fig. 4*B*). These controls, chosen because the cytoplasmic cytohesin-1, has previously been shown to be an important regulator of β2 integrin adhesive function (20, 28, 29), and the aptamer viruses were tested in adhesion assays with these cells as described above. The cytohesin-1 PH+c-domains (cIg-PH+c) had a strongly suppressive effect on PMA-inducible adhesion, whereas neither the isolated PH domain (cIg-PH), which shows considerably reduced phospholipid binding and membrane association (29) nor the control protein had any effect (Fig. 4*C*). These results are in accordance with published data obtained with Jurkat cells (28). Most importantly, Fig. 4*C* also shows that TR-D20 aptamer mediated reduction of PMA-inducible adhesion in PBMC is similar to that observed with cIg-PH+c, whereas the negative control sequence TR-D42 had no effect on β2 integrin-mediated adhesion to ICAM-1. Taken together, these results indicate that the adhesive function of LFA-1 was specifically reduced in Jurkat E6 cells and PBMC by the cytoplasmic expression of an aptamer selected *in vitro* to bind the cytoplasmic portion of the receptor (Fig. 4 *A* and *C*) (15).

To define the binding site of the aptamers on the CD18cyt, gel-shift experiments were performed with three synthetic CD18cyt peptide fragments (Fig. 5). No binding to the C-terminal half of CD18cyt (peptide A23) was observed with any of the aptamers, but TR-D20, TR-D28, and, more weakly, TR-D31 all bound to both the N-terminal peptide B16 and the middle portion C17. B16 and C17 overlap by eight amino acids, including a cluster of three basic arginine residues. That this highly positively charged cluster was selected by the aptamers as a binding site on CD18cyt is not surprising, because an aptamer is a highly negatively charged molecule. As expected, the negative-control aptamer TR-D42 exhibited no binding to any of the three fragments used, confirming that the peptide-fragment recognition is aptamer-specific.

How do our data fit into the current picture of intracellular processes involved in integrin activation? Numerous studies have tried to address the mechanisms involved by mutational analyses of integrin intracellular domains and subsequent functional tests. A related focus of interest has been the biochemical and genetic isolation of cellular factors that bind to integrin receptors from the cytoplasmic side. A variety of proteins have emerged whose interaction sites with the β2 cytoplasmic tail may be targeted by some of the aptamers presented here [e.g., cytohesin-1 (20), α-actinin (18), and filamin (19)]. Indeed, there is some overlap of the aptamer-binding region with the minimal α-actinin-binding sequence in the β2 cytoplasmic tail, but the correlation is not perfect. Future studies will have to investigate whether the aptamers target intracellular processes due to known interactions—if so, our approach will provide an elegant means of testing the relevance of some of these—or whether novel interactions are involved in the observed phenomena.

Most of our current knowledge regarding factors and mechanisms that control integrin activation stems from mutational analyses of integrin domains. This study shows that it is now feasible to address this issue by retaining the genetic integrity of the wild-type CD18 cytoplasmic domain. We established that the intracellular expression of CD18cyt-specific aptamers can affect the functional state of endogenous LFA-1 molecules. Futhermore, we provide evidence that these "intramers" target a specific subdomain of the β2 cytoplasmic tail, implicating this region as important for the proper function of the endogenous LFA-1 receptor with respect to its adhesion to ICAM-1. Above all, we have shown that it is possible to express high levels of functional *in vitro*-selected RNA aptamers in the cytoplasm of eukaryotic cells. Our data demonstrate that cytoplasmic aptamers are capable of targeting receptors that are anchored in the plasma membrane compartment, thus opening an even wider application potential for aptamer technology compared with what are already a number of significant studies on nuclear aptamer expression (30–32) or translational regulation (33).

We thank W. Nagel, C. Geiger, D. Proske, A. Jenne, and E.-L. Winnacker for discussions and support, J. W. Szostak for helpful comments on the manuscript, C. Huber for excellent technical assistance, B. Seed for the vT7, and Vaclav Horeijsi for antibody MEM-170. This work was supported by grants from the Deutsche Forschungsgemeinschaft, and the Fonds der Chemischen Industrie (to M.F.).

1. Spencer, D. M., Wandless, T. J., Schreiber, S. L. & Crabtree, G. R. (1993) *Science* **262,** 1019–1024.
2. Vidal, M., Brachmann, R. K., Fattaey, A., Harlow, E. & Boeke, J. D. (1996) *Proc. Natl. Acad. Sci. USA* **93,** 10315–10320.
3. Colas, P., Cohen, B., Jessen, T., Grishina, I., McCoy, J. & Brent, R. (1996) *Nature (London)* **380,** 548–550.
4. Huang, J. & Schreiber, S. L. (1997) *Proc. Natl. Acad. Sci. USA* **94,** 13396–13401.
5. Rondon, I. J. & Marasco, W. A. (1997) *Annu. Rev. Microbiol.* **51,** 257–283.
6. Ellington, A. D. & Szostak, J. W. (1990) *Nature (London)* **346,** 818–822.
7. Tuerk, C. & Gold, L. (1990) *Science* **249,** 505–510.
8. Joyce, G. F. (1994) *Curr. Opin. Struct. Biol.* **4,** 331–336.
9. Gold, L., Polisky, B., Uhlenbeck, O. & Yarus, M. (1995) *Annu. Rev. Biochem.* **64,** 763–797.
10. Osborne, S. E. & Ellington, A. D. (1997) *Chem. Rev.* **97,** 349–370.
11. Famulok, M. & Jenne, A. (1998) *Curr. Opin. Chem. Biol.* **2,** 320–327.
12. Hynes, R. O. (1992) *Cell* **69,** 11–25.
13. Diamond, M. S. & Springer, T. A. (1994) *Curr. Biol.* **4,** 506–517.
14. Dedhar, S. & Hannigan, G. E. (1996) *Curr. Opin. Cell Biol.* **8,** 657–669.
15. Lub, M., van Kooyk, Y. & Figdor, C. G. (1995) *Immunol. Today* **16,** 479–483.
16. Stewart, M. P., McDowall, A. & Hogg, N. (1998) *J. Cell Biol.* **140,** 699–707.
17. Hibbs, M. L., Jakes, S., Stacker, S. A., Wallace, R. W. & Springer, T. A. (1991) *J. Exp. Med.* **174,** 1227–1238.
18. Pavalko, F. M. & LaRoche, S. M. (1993) *J. Immunol.* **151,** 3795–3807.
19. Sharma, C. P., Ezzell, R. M. & Arnaout, M. A. (1995) *J. Immunol.* **154,** 3461–3470.
20. Kolanus, W., Nagel, W., Schiller, B., Zeitlmann, L., Godar, S., Stockinger, H. & Seed, B. (1996) *Cell* **86,** 233–242.
21. Klug, S. J., Hüttenhofer, A., Kromayer, M. & Famulok, M. (1997) *Proc. Natl. Acad. Sci. USA* **94,** 6676–6681.
22. Famulok, M. (1994) *J. Am. Chem. Soc.* **116,** 1698–1706.
23. Coligan, J. E., Kruisbeek, A. M., Margulies, D. H., Shevach, E. M. & Strober, W. (1994) *Current Protocols in Immunology* (Wiley, New York).
24. Romeo, C. & Seed, B. (1991) *Cell* **64,** 1037–1046.
25. Falkner, F. G. & Moss, B. (1988) *J. Virol.* **62,** 1849–1854.
26. Asubel, F. M., Brent, R., Kingston, R. E., Moore, D. D., Seidman, J. G., Smith, J. A. & Struhl, K., eds. (1987) *Current protocols in Molecular Biology* (Wiley, New York).
27. Fuerst, T. R. & Moss, B. (1989) *J. Mol. Biol.* **206,** 333–348.
28. Nagel, W., Zeitlmann, L., Schilcher, P., Geiger, C., Kolanus, J. & Kolanus, W. (1998) *J. Biol. Chem.* **273,** 14853–14861.
29. Nagel, W., Schilcher, P., Zeitlmann, L. & Kolanus, W. (1998) *Mol. Biol. Cell* **9,** 1981–1994.
30. Symensma, T. L., Giver, L., Zapp, M., Takle, G. B. & Ellington, A. D. (1996) *J. Virol.* **70,** 179–187.
31. Good, P. D., Krikos, A. J., Li, S. X., Bertrand, E., Lee, N. S., Giver, L., Ellington, A., Zaia, J. A., Rossi, J. J. & Engelke, D. R. (1997) *Gene Ther.* **4,** 45–54.
32. Thomas, M., Chedin, S., Carles, C., Riva, M., Famulok, M. & Sentenac, A. (1997) *J. Biol. Chem.* **272,** 27980–27986.
33. Werstuck, G. & Green, M. R. (1998) *Science* **282,** 296–298.